

Characterization of Drag Reducing Guar Gum in a Rotating Disk Flow

C. A. KIM,¹ S. T. LIM,¹ H. J. CHOI,¹ J.-I. SOHN,² M. S. JHON³

¹ Department of Polymer Science and Engineering, Inha University, Incheon, 402-751, Korea

² Department of Chemistry, Hallym University, Chunchon, 200-702, Korea

³ Department of Chemical Engineering, Carnegie Mellon University, Pittsburgh, Pennsylvania 15213

Received 22 February 2000; accepted 29 May 2001

ABSTRACT: The turbulent drag reduction characteristics in a rotating disk apparatus were investigated by using polysaccharide guar gum in deionized water. The ultrasonic degradation method was adopted to obtain different molecular weight fractions of guar gum for this study. The stability of guar gum over time was observed to be better than the typical synthetic water-soluble drag reducers [e.g., poly(ethylene oxide)]. A linear correlation between polymer concentration and the concentration/(drag reduction) for different molecular weights of guar gum was obtained, and the universal drag reduction curve for the guar gum/deionized water system was constructed. © 2002 John Wiley & Sons, Inc. *J Appl Polym Sci* 83: 2938–2944, 2002; DOI 10.1002/app.10300

Key words: drag reduction; turbulence; rotating disk apparatus; degradation; polysaccharide; guar gum

INTRODUCTION

Drag reduction (DR) by injection of a minute amount of high-molecular-weight polymeric additives in turbulent flow, which reduces the pressure drop for a given flow rate, was the subject of intensive theoretical and experimental research because of its wide range of applications,^{1–3} including crude oil transportation,⁴ fire fighting,⁵ hydraulic transportation of solid particle suspensions,⁶ and enhanced ocean thermal energy conversion systems.⁷

DR is known to be strongly influenced by the molecular parameters of the dissolved polymers and the solvent. Therefore, investigations corre-

lating the DR with molecular parameters were widely attempted. Virk et al.⁸ observed the extent of DR for pipe flow of a polyethylene oxide (PEO) in the water system and constructed a universal DR curve, which was later modified by Little.⁹ The universal drag reduction equation depends only on the polymer/solvent pairing and is independent of the molecular weight and flow geometry. Gramain and Borreill¹⁰ found that the universal curve is only satisfied for very low concentration, depending on the molecular weight and on the Reynolds number, and maximum DR varies with the molecular weight and polydispersity.

The most efficient drag reducers are known to be soluble, flexible, linear, and high-molecular-weight polymers. However, the use of these flexible, high-molecular-weight polymers is limited because of their susceptibility to flow-induced shear degradation. To overcome this limitation, there were various attempts for selecting more

Correspondence to: H. J. Choi (hjchoi@inha.ac.kr).

Contract grant sponsor: Korea Science and Engineering Foundation.

Journal of Applied Polymer Science, Vol. 83, 2938–2944 (2002)
© 2002 John Wiley & Sons, Inc.

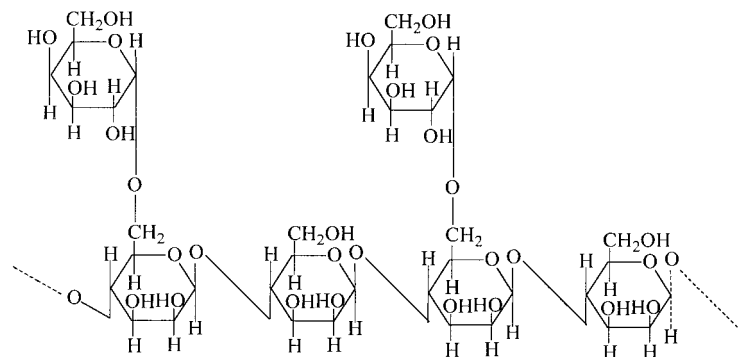


Figure 1 Chemical structure of GG.

efficient, shear, stable polymers. Kim et al.¹¹ observed that branched polyacrylamide (PAAM) is more shear stable than linear PAAM. Similar results by Singh et al.^{12,13} showed that graft copolymers of PAAM and xanthan gum (XG) are fairly shear stable. On the basis of these studies, it is suggested that introducing branches to the rigid backbones will yield increased mechanical/shear stability. Therefore, characterization of backbone polymers using graft copolymerization is needed. Certain industrial polysaccharides such as XG, guar gum (GG), and carboxymethyl cellulose usually were used as backbones. XG-based polymers were found to be fairly shear stable, drag reducers. Kim et al.¹⁴ studied the effects of XG concentration on drag reduction and characterized its drag-reducing efficiency.

In this study, we investigate the drag reduction characteristics of GG as a potential candidate for a shear stable drag reducer by using a rotating disk apparatus (RDA). The RDA system is used to describe external flow that includes the flow over flat plates as well as the flow around immersed objects.¹⁵ DR only affects the friction drag. Friction drag is measured for an internal flow (e.g., pipe flow),¹⁶ whereas total drag (friction plus form drag) is measured for an external flow (e.g., RDA).

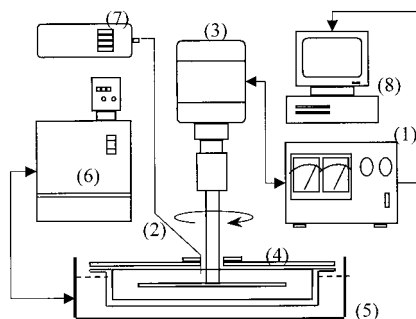
EXPERIMENTAL

The GG used in this experiment was obtained from the Sigma Chemical Co. (St. Louis, MO). GG, which is water-soluble, is a galactomannan polysaccharide,¹⁷ consisting of linear chains of 1,4-linked β-D-mannopyranosyl units with α-D-galactopyranosyl units attached by 1,6-links in a ratio of 2 : 1, which is found in the seed of the guar

plant. The chemical structure of GG is shown in Figure 1. We used it without any purification or treatment by any bactericides.

Because only a single molecular weight of GG is commercially available, the ultrasonic degradation method was adopted to make several different molecular-weight fractions of GG. The ultrasonic degradation method was widely used to obtain several fractionated samples of polysaccharides without any structural or chemical modification.^{14,18} Sample solutions, which were prepared at 0.5 wt % concentration by mildly stirring for 1 week in deionized water, were exposed to 750 W of sound at 28 kHz with a custom-designed ultrasonicator for a specified time to achieve the desired chain scission. Three samples with different molecular weights, such as unsonicated virgin guar gum (GGV), guar gum ultrasonicated for 30 min (GG30), and guar gum ultrasonicated for 60 min (GG60), were obtained.

The RDA was the same as previously reported,^{14,19–21} in which we examined the characteristic drag-reducing behaviors of polysaccharide xanthan gum¹⁴ and PEO.¹⁹ To analyze turbulent drag reduction, most research groups have adopted pipe flows, which produce a pressure-driven flow in an enclosed channel. In contrast, we developed an RDA to measure drag reduction. RDA systems were used for measuring both the mechanical shear degradation of polymeric materials and the frictional reduction.^{14,19,22–27} The flow in the neighborhood of a rotating disk is of great practical importance, particularly in connection with rotary machines. In addition, because the rotating disk flow is drag flow with no imposed pressure gradients, the origin of the turbulent boundary layer is different than in the pressure-driven flow case. The RDA system, in-



(1) speed controller, (2) thermocouple, (3) motor, (4) solution container, (5) water bath, (6) water-circulating system, (7) thermometer, and (8) PC.

Figure 2 Schematic diagram of a rotating disk apparatus.

terfaced with the computer control unit, combines high-speed data sampling with controlled disk rotational speed to accurately measure fluid friction from laminar to turbulent flow.

The device consists of a stainless steel disk with dimensions 14.5 cm in diameter and 0.32 cm in thickness, enclosed in a cylindrical, temperature-controlled container composed of stainless steel with dimensions 16.3 cm inner diameter and 5.5 cm height. A schematic diagram of the RDA is shown in Figure 2. An electric transducer was used to monitor the torque on the disk rotating at 1800 rpm, yielding a rotational Reynolds number N_{Re} of 9.6×10^5 . Here, N_{Re} is defined as:

$$N_{Re} = \rho r^2 \omega / \mu \quad (1)$$

where ρ is the fluid density, μ is the fluid viscosity, r is the radius of the disk, and ω is the rotational speed of the disk. The kinematic viscosity (μ/ρ) of the polymer solution is measured to be about $0.98 \times 10^{-2} \text{ cm}^2/\text{s}$ from the viscosity obtained from the shear behavior of the fluid, as shown in Figure 3. The density of the fluid was 0.98 g/cm^3 , which is very close to deionized water. With the use of the RDA, turbulence is produced for $N_{Re} > 3 \times 10^5$, or, equivalently, $\omega > 570 \text{ rpm} \times 2\pi$.²⁸ Because the DR phenomenon for the polymer occurs only in the turbulent region, all RDA measurements in our study were taken at 1800 rpm, ensuring that measurements are in the turbulent region. The temperature of the system was maintained at $25 \pm 0.5^\circ\text{C}$, and the volume of solution required to fill the entire container was approximately 1l.

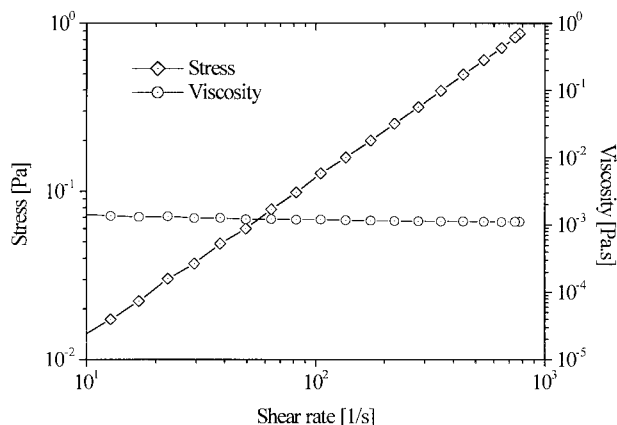


Figure 3 Shear stress and viscosity of GG (200 wppm) in deionized water at 25°C .

Data were taken by measuring the torque required to rotate the disk at a fixed speed both in the pure solvent (T_0) and in a dilute polymer solution (T_p). The percentage drag reduction (%DR) was calculated by:

$$\%DR = \frac{T_0 - T_p}{T_0} \times 100 \quad (2)$$

RESULTS AND DISCUSSION

We examined the effect of polymer concentration (C) on DR efficiency, as shown in Figure 4, which demonstrates the dependence of %DR on the ultrasonication duration of the GG as a function of

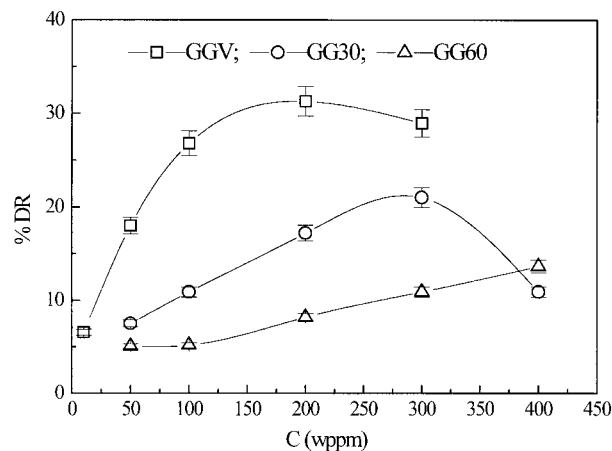


Figure 4 %DR versus GG concentration for three different molecular weights.

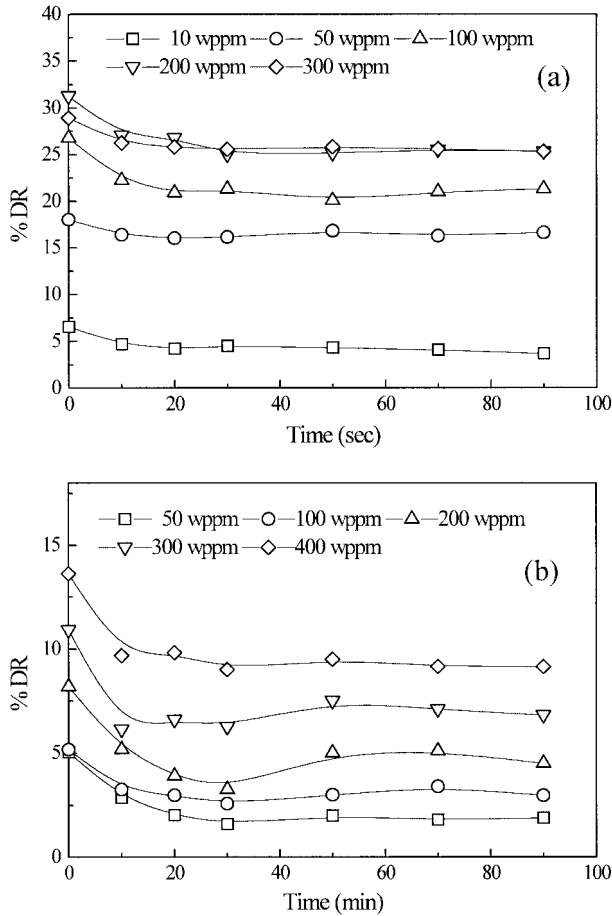


Figure 5 (a) %DR versus time for different concentrations of GG60. (b) %DR versus time for different concentrations of GG60.

C up to 400 wppm at a given rotational speed of 1800 rpm. Maximum values of drag reduction are observed at 200 and 300 wppm for GG60 and GG30, respectively. However, a maximum drag reduction value does not occur for GG60 below 400 ppm. Yang et al.²⁴ observed that the concentration giving maximum drag reduction for the PEO/deionized water system is shifted to a lower value as the molecular weight of PEO increases. Therefore, our observation in Figure 4 that the higher molecular-weight polymer solution shows the maximum drag reduction at lower polymer concentrations is consistent with the PEO/water system.

Mechanical degradation greatly complicates understanding the effect of molecular weight on DR efficiency.²⁹ To study the shear stability or mechanical degradation of polymer chains in turbulent flow, we measured the time-dependent

drag reduction. Figure 5(a,b) depicts the %DR for several polymer concentrations as a function of time for GG60 and GG30, respectively. To compare the shear stability effects in turbulent flow, we conducted an experiment with a typical synthetic water-soluble drag-reducing polymer, PEO, in seawater at 1800 rpm (same conditions). As shown in Figure 6, the drag reduction decreases as a function of time and then levels off. The PEO solution is more effective than GG because a lower concentration is required for equivalent DR. However, the %DR of the PEO solution drops more than 10% after only 10 min in the RDA. On the other hand, GG solutions show remarkable resistance to shear degradation. As previously mentioned, polysaccharide polymers are known to resist shear degradation.³⁰ Kenis³¹ compared the drag reduction effect of polysaccharides and synthetic polymers and observed that polysaccharide polymers are less influenced by shear stress than synthetic polymers, which is consistent with the observation shown in Figures 5 and 6. It is noted that GG is also more resistant to mechanical degradation than XG.^{14,31}

To test the mechanical degradation of GG, we exposed the GG molecules to the turbulent flow field for a long time. Figure 7 shows the %DR behavior for GG over 10 h with three different molecular weights at 1800 rpm. From the relative drag reduction efficiency, GG solutions exhibit plateau values between 62 and 80% of the initial drag reduction effect, respectively.

Because of the complex nature of the DR phenomenon, rigorous theoretical predictions do not satisfactorily fit experimental data,³² but empirical relationships were developed. A universal

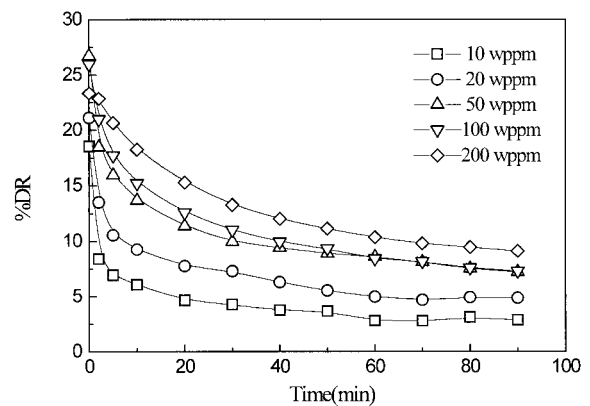


Figure 6 %DR of PEO ($M_w: 4 \times 10^6$) versus time for various PEO concentrations.

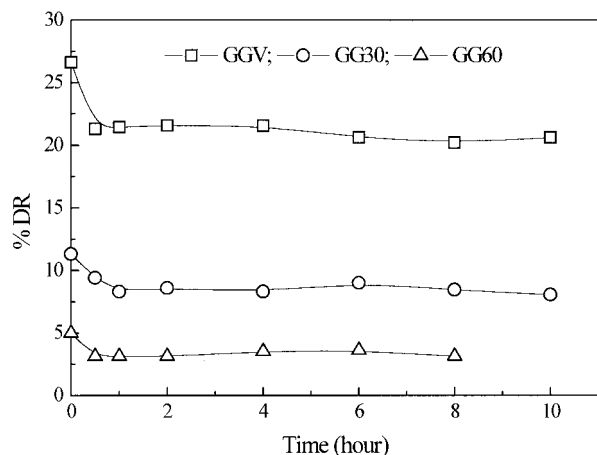


Figure 7 %DR versus time for a 100 wppm GG solution.

drag reduction equation developed by Virk⁸ and reformulated by Little⁹ accounts for the concentration dependence on DR. In addition, Choi and Jhon²² obtained a similar universal relationship by using a three-parameter correlation. Recently, Kim et al.¹⁴ adapted this equation for any system in the form:

$$\frac{C}{\overline{DR}} = \frac{K[C]}{\overline{DR}_{\max}} + \frac{C}{\overline{DR}_{\max}} \quad (3)$$

where C is in wppm, K is a parameter depending on the polymer/solvent system, \overline{DR}_{\max} is the maximum drag reduction, and $[C]$ is the intrinsic concentration. \overline{DR}_{\max} can be used to define the intrinsic drag reduction; $[\overline{DR}]$ is as follows:

$$[C] = \frac{\overline{DR}_{\max}}{\lim_{C \rightarrow 0} \left(\frac{\overline{DR}}{C} \right)} \quad (4a)$$

$$[\overline{DR}] = \frac{\overline{DR}_{\max}}{[C]} = \lim_{C \rightarrow 0} \frac{\overline{DR}}{C} \quad (4b)$$

Better drag reducing agents exhibit lower values of intrinsic concentration. Equation (3) is valid for a given Reynolds number and also shows that there is a linear relationship between C/\overline{DR} and C up to the optimum concentration for a given molecular weight. This is also valid for most drag-reducing polymers in pipe flow^{8,9} and rotating disk flow.^{14,19} The linear relationship between

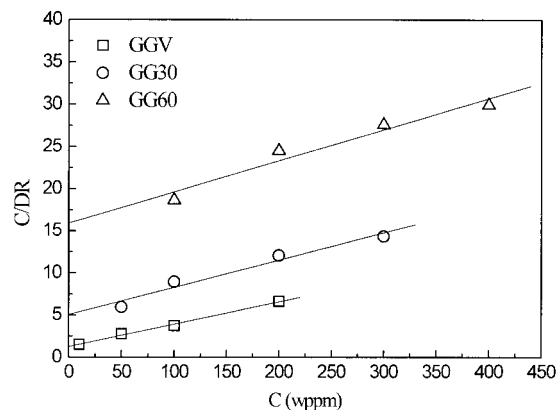


Figure 8 Concentration dependence of DR for various ultrasonication times of GG.

C/\overline{DR} and C for three different GG molecular weights, obtained by controlling the duration of the ultrasonication, is illustrated in Figure 8 up to the polymer concentration, giving the maximum drag reduction. \overline{DR}_{\max} is obtained from the reciprocal of the slope given in Figure 8; $[C]$ is obtained by multiplying the intercept by \overline{DR}_{\max}/K . More efficient drag reducers³³ are known to have a higher \overline{DR}_{\max} and a smaller $[C]$. Moreover, $[C]$ was found to be extremely useful in normalizing the drag reduction results for different molecular weights into one homologous series, as shown in Figure 9. If we define $(\overline{DR}/C)/[\overline{DR}]$ as β and $C/[C]$ as α , eq. (3) can be written as a universal curve with a single parameter K :

$$\beta = \frac{1}{K + \alpha} \quad (5)$$

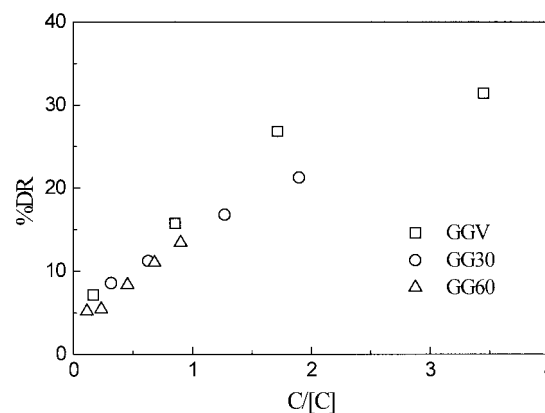


Figure 9 %DR versus $C/[C]$ for GG in deionized water at 1800 rpm.

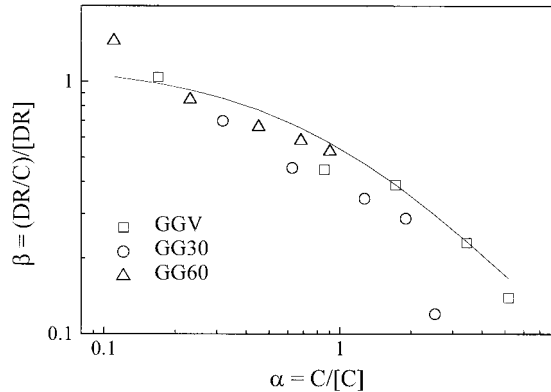


Figure 10 Universal drag reduction curve, β versus α , for fractionated GG in deionized water ($K = 0.85$).

Figure 10 infers that the universal curve equation for GG in deionized water using the RDA is independent of the polymer molecular weight. This also indicates that $(DR/C)/[DR]$ possesses a very strong universal correlation with $C/[C]$, as given in eq. (5). K is calculated to be 0.85 for the GG system with R^2 (correlation coefficient) = 0.81 from the nonlinear curve-fitting method using a plotting program. The value of K is 1 for the PEO–water in a pipe flow system.⁸ In a different geometry, such as a RDA, K is also 1 for the PEO–water system.²² For a PIB–toluene system, Dschagarowa and Mennig³⁴ obtained the universal curve $\beta = 1/(0.4 + \alpha)$ using a capillary tube. From these results, K becomes a constant parameter inherent to the interaction between a given polymer/solvent pair. Therefore, the constant K is considered a characteristic of a particular polymer/solvent system and does not depend on the molecular weight or the flow geometry. In addition, the numerical value of K is observed to be 1.2 for other polysaccharides, such as XG, in a deionized water system.¹⁴

CONCLUSION

We examined the DR efficiency of GG in deionized water by using an RDA and found that GG is a useful, water-soluble drag reducer, more resistant to the mechanical stress than the synthetic, water-soluble drag reducer, PEO. The linear correlation between C and C/DR for GG is obtained in the RDA system. In addition, we constructed a universal correlation to characterize the drag reduction of GG and confirmed that K is a charac-

teristic constant of a particular polymer/solvent system and does not depend on the molecular weight, giving 0.85 for the GG in the deionized water system.

This study was supported by research grants from the Korea Science and Engineering Foundation (KOSEF) through the Applied Rheology Center (ARC), an official KOSEF-created engineering research center (ERC) at Korea University, Korea.

REFERENCES

1. Armstrong, R.; Jhon, M. S. *Chem Eng Commun* 1984, 30, 99.
2. Kulicke, W.-M.; Kötter, M.; Gräger, H. *Adv Polym Sci* 1989, 89, 1.
3. Tong, P.; Goldburg, W. I.; Huang, J. S.; Witten, T. A. *Phys Rev Lett* 1990, 65, 2780.
4. Burger, E. D.; Chorn, L. G. *J Rheol* 1980, 24, 603.
5. Fabular, A. G. *Trans ASME J Basic Eng* 1971, 93, 453.
6. Golda, J. *Chem Eng Commun* 1986, 45, 53.
7. Kim, C. A.; Sung, J. H.; Choi, H. J.; Kim, C. B.; Chun, W.; Jhon, M. S. *J Chem Eng Jpn* 1999, 32, 803.
8. Virk, P. S.; Merrill, E. W.; Mickley, H. S.; Smith, K. A.; Christensen, E. L. *J Fluid Mech* 1967, 30 (2), 305.
9. Little, R. C. *J Colloid Interface Sci* 1971, 37 (4), 811.
10. Gramain, Ph.; Borreill, J. *Rheol Acta* 1978, 17, 303.
11. Kim, O. K.; Little, R. C.; Patterson, R. L.; Ting, R. Y. *Nature* 1974, 250, 408.
12. Deshmukh, S. R.; Singh, R. P. *J Appl Polym Sci* 1986, 32, 6163.
13. Ungeheuer, S.; Bewersdorff, H.-W.; Singh, R. P. *J Appl Polym Sci* 1989, 37, 2933.
14. Kim, C. A.; Choi, H. J.; Kim, C. B.; Jhon, M. S. *Macromol Rapid Commun* 1998, 19, 419.
15. Kim, C. A.; Jo, D. S.; Choi, H. J.; Kim, C. B.; Jhon, M. S. *Polym Test* 2001, 20, 43.
16. Kim, N. J.; Lee, J. Y.; Yoon, S. M.; Kim, C. B.; Hur, B. K. *J Ind Eng Chem* 2000, 6, 412.
17. Budavari, S.; O'Neil, M. J.; Smith, A.; Heckelman, P. E. *The Merck Index*, 11th ed.; Merck and Co.: Rahway, NJ, 1989; p 4484.
18. Chun, M. S.; Park, O. O. *Macromol Chem Phys* 1994, 195, 701.
19. Choi, H. J.; Kim, C. A.; Jhon, M. S. *Polymer* 1999, 40, 4527.
20. Choi, H. J.; Kim, C. A.; Sohn, J. I.; Jhon, M. S. *Polym Degrad Stab* 2000, 69, 341.
21. Sohn, J. I.; Kim, C. A.; Choi, H. J.; Jhon, M. S. *Carbohydr Polym* 2001, 45, 61.

22. Choi, H. J.; Jhon, M. S. *Ind Eng Chem Res* 1996, 35, 2993.
23. Kim, C. A.; Lee, K.; Choi, H. J.; Kim, C. B.; Kim, K. Y.; Jhon, M. S. *J Macromol Sci, Pure Appl Chem* 1997, A34, 705.
24. Yang, K. S.; Choi, H. J.; Kim, C. B.; Kim, I. S.; Jhon, M. S. *Korean J Chem Eng* 1994, 11, 8.
25. Rodriguez, F.; Wing, C. C. *Ind Eng Chem* 1959, 51, 1281.
26. Hoyt, J. W. *Trans ASME J Basic Eng* 1972, 94, 258.
27. Mumick, P. S.; Welch, P. M.; Salzar, L. C.; McCormick, C. L. *Macromolecules* 1994, 27, 323.
28. Schlichting, H. *Boundary Layer Theory*, 7th ed.; McGraw-Hill: New York, 1979.
29. Kim, C. A.; Kim, J. T.; Lee, K.; Choi, H. J.; Jhon, M. S. *Polymer* 2000, 41, 7611.
30. Bello, J. B.; Müller, A. J.; Sáez, A. E. *Polym Bull* 1996, 36, 111.
31. Kenis, P. R. *J Appl Polym Sci* 1971, 15, 607.
32. Paireau, O.; Bonn, D. *Phys Rev Lett* 1999, 83, 5591.
33. Hunston, D. L.; Zakin, J. L. *Polym Eng Sci* 1980, 20, 517.
34. Dschagarowa, E.; Menning, G. *Rheol Acta* 1977, 16, 309.